Progress in Engineering Application and Technology Vol. 1 No.1 (2020) 438-447

PEAT

Homepage: http://publisher.uthm.edu.my/periodicals /index.php/peat
e-ISSN : 0000-0000

Simulation on The Effect of Fluid Velocity on The Flow and Structure Performance of The Pipeline in UTHM Biodiesel Pilot Plant

Norfatihah Abdul Rashid[1], Zuliazura Mohd Salleh[1]*, Rosniza Hussin[1] , Razlin Abd Rashid[1]

[1]Department of Mechanical Engineering Technology, Faculty of Engineering Technology, Universiti Tun Hussein Onn Malaysia Pagoh Campus, KM 1 Jalan Panchor, 84600 Pagoh, Johor, MALAYSIA

*Corresponding Author Designation

DOI: https://doi.org/10.30880/peat.2020.01.01.046
Received 12 September2020; Accepted 12 November 2020; Available online 02 Month 2020

Abstract: Fuels are produced from biological feedstock known as biofuels. Nowadays, biodiesel has been reported to be one of the strong contenders for reductions in exhaust emission because of its more environment friendly and renewable fuels. In biodiesel plant, piping is the most important part because it is the main transport system used to transfer the biodiesel oil from one process to another. The purpose of this study is to investigate the flow behaviour and structure performance effect to the piping line by using three different velocities inlet (0.0100 m/s, 0.0200 m/s and 0.0300 m/s). The outcome of this study is to know which part have the highest possibilities in risk. The main geometry of the piping line was based on UTHM Biodiesel Pilot Plant. This study focused on the piping line from esterification process until trans-esterification process. Simulation was conducted to determine the velocity distribution, pressure and stress. The simulation was done by using ANSYS software. From the simulation, the highest risk occurred at velocity inlet 0.0300 m/s with the maximum stress located at fitting 8 with maximum stress recorded at $2.878e^8$ Pa.

Keywords: CFD, Pipeflow, Stress in Pipe

1. Introduction

Nowadays, biodiesel has been reported to be one of the strong contenders for reductions in exhaust emission because of its more environmentally friendly and renewable fuels [1-5]. Biodiesel is a promising source of renewable energy and a potential future petroleum substitute [6]. In Malaysia, the production of palm oil is the highest compare to the other Asia country. There are many type of biodiesel which are B100, B20, B10 and others. But B100 have the highest demand due to its purities. In biodiesel plant, piping is the primary transport system to transfer the oil from one tank to another. It is required to monitor and recognize the possible risk in the piping line because it can affect production performances. In this study, simulation analysis on the flow and structure behavior was conducted to

*Corresponding author: zulia@uthm.edu.my

see the velocity, pressure and stress distribution. From the results, prediction on the risk along the pipeline were determined.

The geometry of the pipe is according to UTHM Biodiesel Pilot Plant in Universiti Tun Hussen Onn, Batu Pahat, Johor, Malaysia. For this study, it focused on esterification until the trans-esterification process pipe line using three different inlet velocities which are 0.0100 m/s, and 0.0200 m/s and 0.0300 m/s. The main objective is to lay out the possible risk in the pipeline to predict any failure. If the risk is known, the next step, such as maintenance, can ensure the production performance is not disturbed.

1.1 Process Flow of Biodiesel

The study was conducted from esterification until trans-esterification because at that process the biodiesel was started to produce. Biodiesel is synthesized from triglycerides in vegetable oils by transesterification reaction with alcohol. Within this reaction, the oil will react to the alcohol in several conservative, reversible steps to form ester and glycerol [7]. Base catalyzed transesterification requires only low temperature and pressure and produces over 98.0 % conversion yield. The transesterification cycle is the reaction of an alcohol-forming triglyceride (fat/oil) to esters and glycerol. A triglyceride, with three long-chain fatty acids attached, has a glycerin molecule as its base. The essence of the fatty acids bound to the glycerin dictates the characteristics of the fat. The nature of the fatty acids can, in turn, affect the characteristics of the biodiesel [8].

1.2 Piping in Biodiesel Plant

Pipeline are like transporting and carrying the crude oil from one tank to another tank for further processing. Pipe play the important roles in the production of biodiesel in biodiesel plant. When the piping does not maintain in good condition , the productivity can be altered and slow down. So, this study were conducted to know the fluid behaviour and structure performance when different velocities is used. From this, some risk can be predict and be solve to avoid the problems.

1.3 Previous study

Table 1 sumarized the previous study that using simulation and non simulation method to conduct the analysis of flow inside the pipe.

Table 1: Summary of previous studies

No	Author/s	Title	Finding	Simulation
1.	Jung, S. Y., & Chung, Y. M., 2012 [9]	Large-eddy Simulation of Accelerated Turbulent Flow In A Circular Pipe.	The transient flow after the onset of the acceleration was divided into three stages, based on the unsteady skin-friction behaviour.	Yes – Large-eddy Simulation.
2.	De Boer, K., & Bahri, P. A., 2009 [10]	Investigation of Liquid-Liquid Two Phase Flow In Biodiesel Production.	At low velocities, the flow stratifies and at the higher velocities the polar phase becomes dispersed in the continuous non-polar phase.	Yes – ANSYS CFX
3.	Akpan, P. U. *et al.*, 2017 [11]	Modelling and Transient Simulation of Water Flow In Pipelines.	The simulation results that it is reasonably accurate to approximate the air behaviour in air vessel used for water pipeline protection system.	Yes – Wanda Transient Simulation Software.
4.	Qin, Z *et al.*, 2017 [12]	Empirical and Quantitative Study of The velocity Distribution Index of The Perforated	Flow velocity distribution index decreases with the increases in the laying slope and increase with the increase in the length diameter ratio and orifice rate.	No.

5.	Liu, T. *et al*., 2017 [13]	Pipe Outflowing Along A Pipeline. Effect of Fluid Flow on Biofilm Formation and Microbiologically Influenced Corrosion of Pipeline in Oilfield Produced Water.	At the high flow velocity, the surface layer formed on the steel is mainly corrosion products. Corrosion pits can be formed on the steel at the low flow velocity due to microbial attack.	No.
6.	Kumara, W. A. S., 2010 [14]	Computational Study On Non-asymptotic Behaviour of Developing Turbulent Pipe Flow.	The development of the mean velocity field of turbulent pipe flow is non-asymptotic but laminar flow show an asymptotic behaviour. The higher the flow Reynold number is, the further the downstream the centreline mean velocity peak overshoot position moves. As the Reynold number increase, the magnitude of the centreline velocity overshoot reduces.	Yes – ANSYS FLUENT 12.0 Software

2. Methodology

There were two simulation methods used in this study to represent the Fluid-structure Interaction (FSI), which is Fluid Fluent and Static Structural. Both simulations were used ANSYS as the software to simulate all cases. Fluid Fluent and Static Structural were used to investigate the flow behaviour and stress distribution along the pipeline. The pipe structure is sketched by using Solidwork. Both of the simulation methods will be analyzed by input three different values of inlet velocity. Velocity, pressure and stress distribution affected by this variable inlet value were then tabulated and analyzed to come out with prediction risk along the pipeline.

2.1 3D Modelling

The 3D piping line models was drawn based on the UTHM Biodiesel Pilot Plant using SolidWorks Software. The piping sizing had measured directly from UTHM Biodiesel Pilot Plant. In this piping line models, it consists of 14 parts which is taken from the esterification process to transesterification process pipeline. The 3D pipeline model was shown in Figure1.

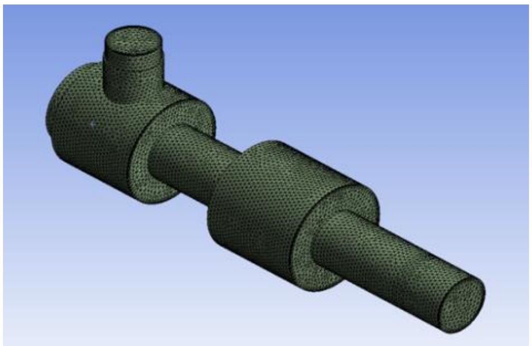

Figure 1: 3D Model of pipeline with 214385 number of meshing elements

The pipeline models then go through a meshing procedure where three different element quantity (55785 elements, 214385 elements and 399647 elements) were applied to test (Grid Independence Test, GIT) the best grid to perform the simulation analysis. The best element quantity chosen was model with 214385 elements which has 67010 nodes.

2.2 Simulation Analysis

Fluid Structure Interaction (FSI) was applied to get more accurate simulation results. This make the results more reliable as the results from the flow analysis effected from different inlet velocities were embedded into the structure analysis.

2.2.1 Simulation for Fluid Flow

Bernoulli Flow Equation

In fluid dynamics, the principle by Bernoulli says that the fluid speed increases at the same time as pressure decreases or the potential energy of the fluid decreases. The fluid speed in the pipe throughout the section is not uniform. A mean speed is used and the continuity equation for the steady flow is calculated as:

$$v= q/A= 4q/(D^2 \pi) \quad \text{(Eq.1)}$$

q – Volumetric flow rate, A – Pipe cross section, D – Internal diameter

Reynold Number

The flow in the pipe may be either laminar or turbulent, depending on the Reynolds number, R and the amount of perturbation. The equation for Reynold number is as

$$R= VD/v=\rho VD/\mu \quad \text{(Eq.2)}$$

Where ρ is the density of the fluid; μ is the dynamic viscosity; v is the kinematic viscosity; V is the cross-sectional mean velocity of the flow in the pipe; and D is the inner diameter of the pipe.

In order to obtain a well-posed system of equation, appropriate boundary conditions for the computational domain have to be implemented such as the inlet velocity and pressure are specified. The fluid parts for piping used in this study was biodiesel B100. The properties of B100 and boundary condition used in the flow analysis were summarized in Table 2.

Table 2: Summary of boundary condition used in fluid domain analysis [8] and [16]

Parameter	**Inlet Velocity (m/s)**		
	0.01 m/s	**0.02 m/s**	**0.03 m/s**
Outlet Pressure (Pa)		101325	
Density (kg/m^3)		878	
Viscosity (mm^2/s)		$5.68e^{-3}$	

2.2.2 Simulation for structure performance

Structural properties for the pipe is include the strain and young modulus. Young's Modulus is the most metal deforms proportional to imposed load over a range of loads. The boundary conditions include the places where the structure interacts with the environment either by applying external forces or by restricting a move. For this study, pressure effected from the flow inside the pipe was applied to the wall of the pipe. Each end of the pipeline were set as fixed point as the pipe originally connected with other components of pipeline that were not included in the analysis. The characteristic for the structure were summarized in Table 2.

Table 3: Summary of boundary condition used in structural domain analysis

Type of pipe	Young's Modulus E, (Pa)	Poisson Ratio
Stainless Steel (304)	$1.93e^{11}$	0.31

3. Results and Discussion

The results of steady state simulation of flow behavior velocity and pressure distribution were discussed and analyzed. The findings are in the form of a contour plot where the particular magnitude of fluid flow is represented by each color. It is possible to evaluate the flow behavior from the magnitude. Here changes in flow behavior can be seen.

3.1 Result for Flow Analysis

Figures in Table 4 below shows the contour of velocity distribution for each inlet velocities

Table 4: Velocity distribution inside the pipeline for three different inlet velocities

	Inlet Velocity	0.01 m/s	0.02 m/s	0.03 m/s
Velocity Distribution	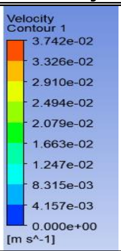	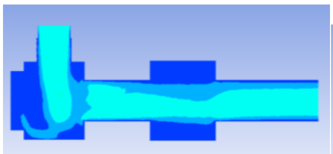	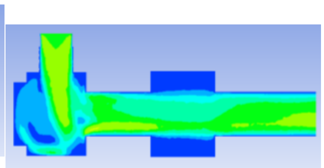	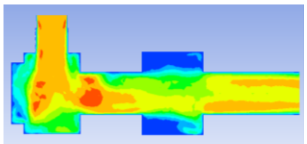

For the inlet velocity of 0.0100 m/s, the maximum velocity in the pipe's fluid domain is 0.0124 m/s. When the inlet velocity is slow, the movement of the flow in the pipe also become slow. For the inlet velocity 0.0200 m/s, the maximum velocity in the fluid domain of the pipe is 0.0234 m/s. For the inlet velocity of 0.0300 m/s, the maximum velocity in the fluid domain of the pipe is 0.0296 m/s. It shows the results produced with different inlet velocities based on figures in Table 4. The flow along with the pipeline increase as the inlet velocities increase. The figure below shows that the contour of each inlet velocities for pressure distribution.

Table 4: Pressure Distribution Inside The Pipeline for Three Different Inlet Velocities

	Inlet Velocity	0.01 m/s	0.02 m/s	0.03 m/s
Pressure Distribution	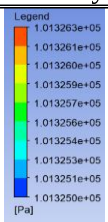	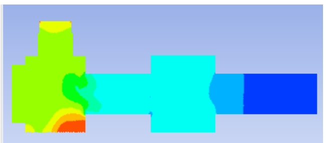	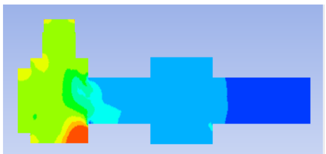	

For the pressure result, when the velocity increases, the pressure distribution also increases. It is found that the third velocity which is 0.0300 m/s has the highest pressure distribution along the pipe. Outlet pressure was fixed at 101325 Pa and the pressure distribution were varied along the pipe. As the pressure distribution varies, the flow layers onto another and the number of Reynolds is calculated to be in the laminar flow range. Therefore, if changing the outlet pressure does not change the flow behavior significantly.

3.2 Result for structure analysis

The figure below shows the stress distribution at the pipeline wall effected from three different velocities inlet.

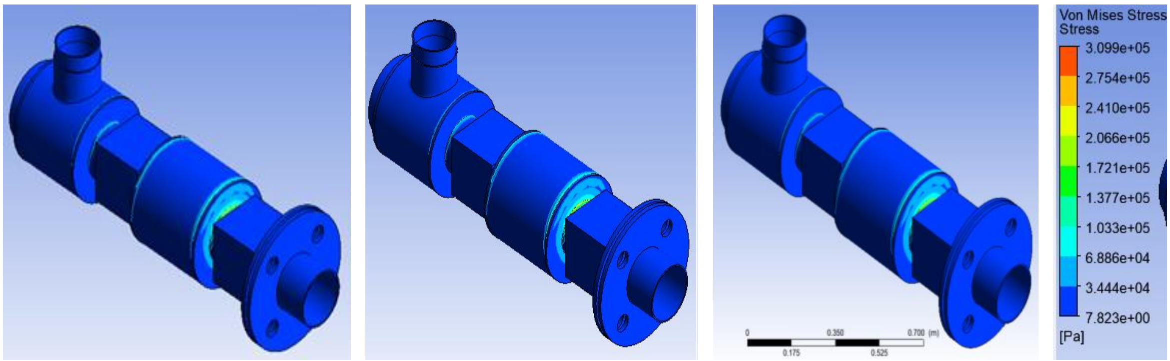

Figure 2: (a) Stress distribution at 0.0100 m/s, (b) Stress distribution at 0.0200 m/s and (c) Stress distribution at 0.0300 m/s

Figure 2 shows that the stress distribution of three inlet velocity has a different minimum and maximum value. It is because the flow does not flow smoothly throughout the fitting in the pipe. In each fitting there are different stress value. For all cases shown in Figure 2, the minimum stress value is 7.823 Pa and the maximum value is $3.099e^5$ Pa. From this result, for inlet velocity, 0.0300 m/s have the highest value of stress. When the inlet velocity is fast, the stress distribution to the wall is highest compare to the other two inlet velocity

3.3 Risk Indicator

No.	V1	V2	V3
1.	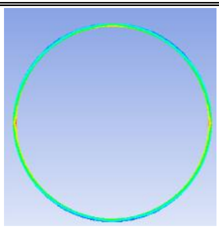 $\min = 17392.5Pa$ $\max = 31112.3Pa$	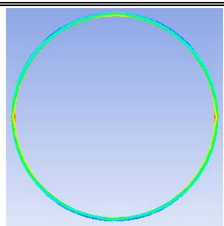 $\min = 17433.2Pa$ $\max = 31179.0Pa$	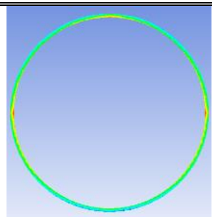 $\min = 1.573e^7 Pa$ $\max = 3.021e^7 Pa$
2.	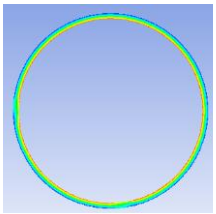 $\min = 1817.43Pa$ $\max = 1986.6Pa$	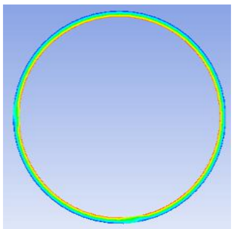 $\min = 1820.96Pa$ $\max = 1990.34Pa$	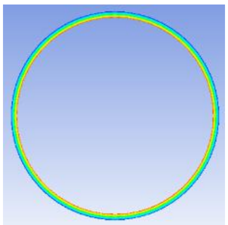 $\min = 1.722e^6 Pa$ $\max = 1.928e^6 Pa$
3.	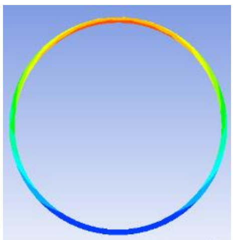 $\min = 2003.82Pa$ $\max = 92733.6Pa$	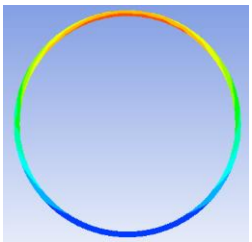 $\min = 2011.92Pa$ $\max = 93020.4Pa$	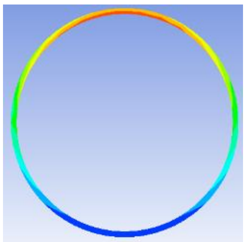 $\min = 1.983e^6 Pa$ $\max = 8.942e^7 Pa$

4.	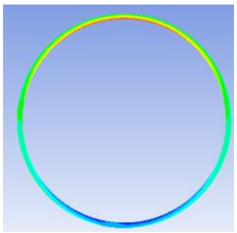 $\min = 955.508Pa$ $\max = 10436.3Pa$	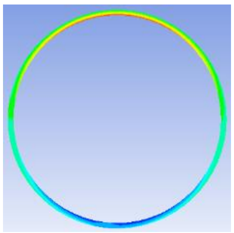 $\min = 962.826Pa$ $\max = 10469.5Pa$	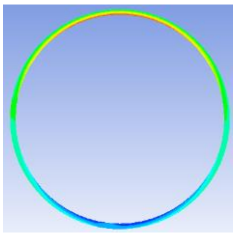 $\min = 0.987e^{6}Pa$ $\max = 1.031e^{7}Pa$
5.	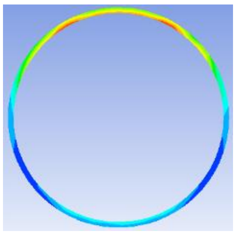 $\min = 2837.10Pa$ $\max = 55079.5Pa$	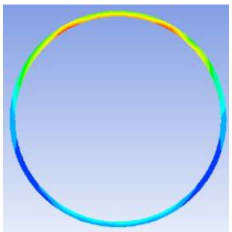 $\min = 2828.67Pa$ $\max = 55275.8Pa$	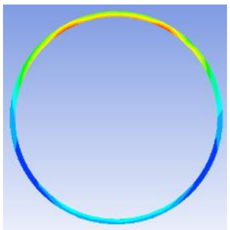 $\min = 2.836e^{6}Pa$ $\max = 5.284e^{7}Pa$
6.	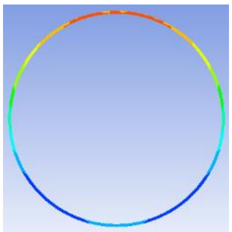 $\min = 2842.29Pa$ $\max = 97717.9Pa$	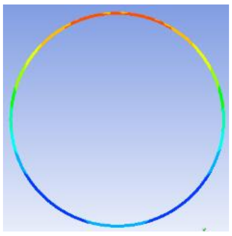 $\min = 2879.10Pa$ $\max = 98034.3Pa$	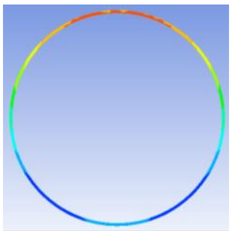 $\min = 2.833e^{6}Pa$ $\max = 9.550e^{7}Pa$
7.	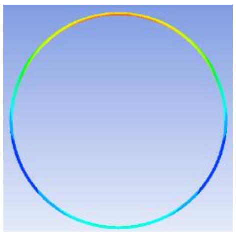 $\min = 7427.98Pa$ $\max = 100063Pa$	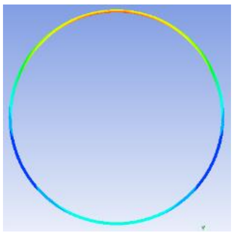 $\min = 7449.77Pa$ $\max = 100430Pa$	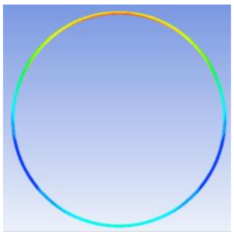 $\min = 7.390e^{6}Pa$ $\max = 1.018e^{8}Pa$
8.	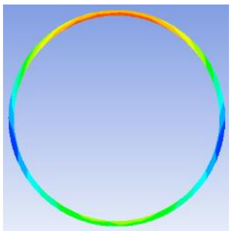 $\min = 12964.1Pa$ $\max = 288727Pa$	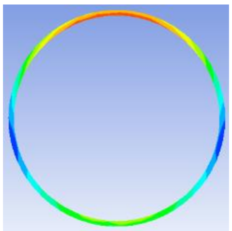 $\min = 13018.9Pa$ $\max = 289904Pa$	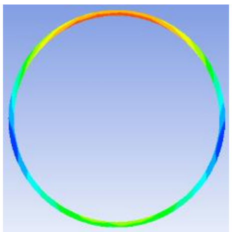 $\min = 1.293e^{7}Pa$ $\max = 2.878e^{8}Pa$

9.	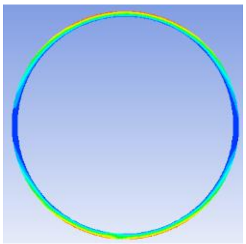 $\min = 4034.42 Pa$ $\max = 28365.1 Pa$	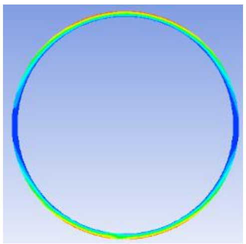 $\min = 4050.06 Pa$ $\max = 284979 Pa$	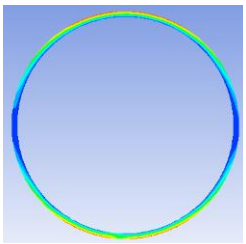 $\min = 4.035 e^{6} Pa$ $\max = 2.829 e^{7} Pa$
10.	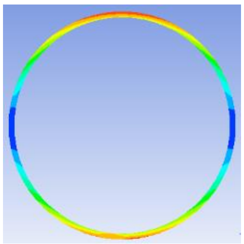 $\min = 1571.80 Pa$ $\max = 18686.7 Pa$	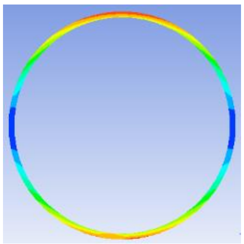 $\min = 1575.70 Pa$ $\max = 18772.3 Pa$	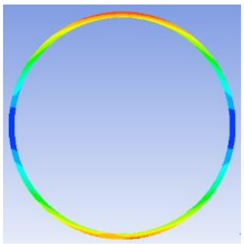 $\min = 1.570 e^{6} Pa$ $\max = 1.866 e^{7} Pa$
11.	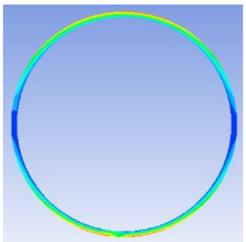 $\min = 1252.76 Pa$ $\max = 28792.6 Pa$	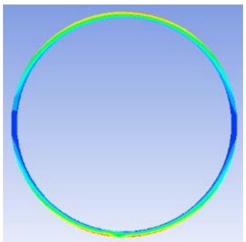 $\min = 1288.46 Pa$ $\max = 28931.2 Pa$	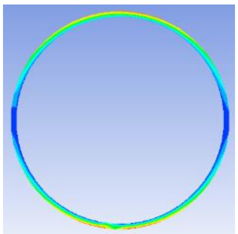 $\min = 1.415 e^{6} Pa$ $\max = 2.841 e^{7} Pa$
12.	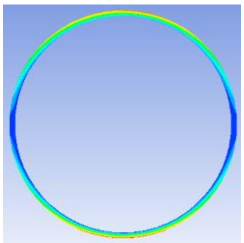 $\min = 1337.49 Pa$ $\max = 28554.5 Pa$	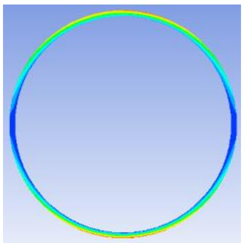 $\min = 1343.01 Pa$ $\max = 28687.0 Pa$	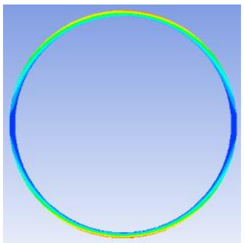 $\min = 1.337 e^{6} Pa$ $\max = 2.849 e^{7} Pa$
13.	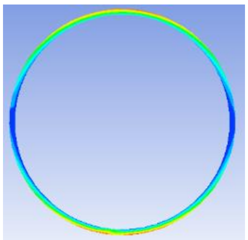 $\min = 2806.29 Pa$ $\max = 27231.5 Pa$	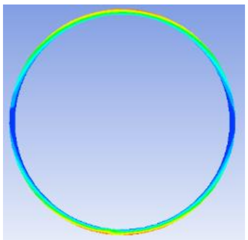 $\min = 2818.77 Pa$ $\max = 27306.3 Pa$	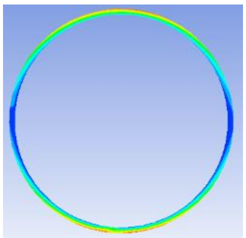 $\min = 3.042 e^{6} Pa$ $\max = 2.634 e^{7} Pa$

From this risk indicator, it shown that the highest risk occur at inlet velocity 0.03 m/s at fitting 8 compare to the other inlet velocities and fittings. When at fitting that have the highest risk, the pipe need to be change frequently because some complication may occur during the process. The results show that the increase in wall stress caused by the high flow velocity leads to the increasing corrosion rate.

4. Conclusion

This study was carried out to know the fluid behaviour and structure behaviour in the pipeline. This research was conducted from esterification until the trans-esterification piping process. The geometry was based on UTHM Biodiesel Pilot Plant at Batu Pahat. Three different velocities inlet were varies to see the effect: 0.0100 m/s, 0.0200 m/s and 0.0300 m/s. The highest stress distribution obtained from the study was at fitting 8 which is for 0.0300 m/s of inlet velocity. So, it can be concluded that if the Biodiesel Plant running the plant operation with the inlet velocity 0.3000 m/s, the possibility for fitting 8 to be breakdown is higher than the other fitting. Thus, maintenance should be scheduled for this fitting as a safety precaution. Overall, the lifespan of the piping line can be predicted as it shows the stress distribution along the pipeline especially at all connections of pipe fittings. This risk assessment can be used as an early diagnosis to plan preventive maintenance so that the biodiesel plant's operation will not be interrupted.

Acknowledgement

The authors would like to thank the Faculty of Engineering Technology, Universiti Tun Hussein Onn Malaysia for its support.

References

[1] Demirbaş, A. (2002). Biodiesel from vegetable oils via transesterification in supercritical methanol. Energy conversion and management, 43(17), 2349-2356.

[2] Demirbas, A. (2008). Production of biodiesel from tall oil. Energy Sources, Part A, 30(20), 1896-1902.

[3] Demirbas, A. (2009). Biofuels securing the planet’s future energy needs. Energy Conversion and Management, 50(9), 2239-2249.

[4] Balat, M. (2007). Production of biodiesel from vegetable oils: A survey. Energy Sources, Part A, 29(10), 895-913.

[5] Nas, B., & Berktay, A. (2007). Energy potential of biodiesel generated from waste cooking oil: an environmental approach. Energy Sources, Part B: Economics, Planning, and Policy, 2(1), 63-71.

[6] Petchmala, A., Laosiripojana, N., Jongsomjit, B., Goto, M., Panpranot, J., Mekasuwandumrong, O., & Shotipruk, A. (2010). Transesterification of palm oil and esterification of palm fatty acid in near-and super-critical methanol with SO4–ZrO2 catalysts. Fuel, 89(9), 2387-2392.

[7] Thomson, I. S. I. (2009). An Alkabbashi, Md Z. Alam, MES Mirgahani and AMA Al-Fusaiel. Journal of Applied Sciene 9. No. 17 (2009): 3166 - 3170.

[8] Sapuan, N. F. (2014). Modelling and Simulation of Flow Behavior through Millichannel Reactor for Biodiesel Production Using CFD.

[9] Jung, S. Y., & Chung, Y. M. (2012). Large-eddy simulation of accelerated turbulent flow in a circular pipe. International Journal of Heat and Fluid Flow, 33(1), 1 - 8.

[10] De Boer, K., & Bahri, P. A. (2009). Investigation of liquid-liquid two phase flow in Biodiesel Production.

[11] Akpan, P. U., Jones, S., Eke, M. N., & Yeung , H. (2017). Modelling and transient simulation of water flow in pipelines using WANDA Trasient software. Ain Shams Engineering Journal, 8(3), 457 – 466.

[12] Qin, Z., Liu, H., & Wang, Y. (2017). Empirical and quantitative study of the velocity distribution index of the perforated pipe outflowing along a pipeline. Flow Measurement and Instrumentation, 58, 46-51.

[13] Liu, T., Cheng, Y. F., Sharma, M., & Voordouw, G. (2017). Effect of fluid flow on biofilm formation and microbiologically influenced corrosion of pipelines in oilfield produced water. Journal of Petroleum Science and Engineering, 156, 451-459.

[14] Kumara, W. A. S., Halvorsen, B. M., & Melaaen, M. C. (2010). Computational study on non-asymptotic behaviour of developing turbulent pipe flow. Advances in Fluid Mechanics VIII, 69, 39-52.

[15] Mat Yasin, M. H., Mamat, R., Yusop, A. F., Rahim, R., Aziz, A., & Shah, L. A. (2013). Fuel physical characteristics of biodiesel blend fuels with alcohol as additives. Procedia Engineering, 53, 701-706.